Classifying Cognitive Impairment Based on the Spatial Heterogeneity of Cerebral Blood Flow Images

Zahra Shirzadi, MESc,[1,2]* Bojana Stefanovic, PhD,[1,2] Henri J.M.M. Mutsaerts, MD, PhD,[2,3]

Mario Masellis, MD, PhD,[2,4] and Bradley J. MacIntosh, PhD,[1,2]

for the Alzheimer's Disease Neuroimaging Initiative

Background: The spatial coefficient of variation (sCoV) of arterial spin-labeled (ASL) MRI can index cerebral blood flow spatial heterogeneity. This metric reflects delayed blood delivery—seen as a hyperintense ASL signal juxtaposed by hypointense regions.

Purpose: To investigate the use of ASL-sCoV in the classification of cognitively unimpaired (CU), mild cognitive impairment (MCI), and Alzheimer's disease (AD) cohorts.

Study Type: Prospective/cohort.

Population: Baseline ASL images from AD neuroimaging initiative dataset in three groups of CU, MCI, and AD (N = 258).

Field Strength/Sequence: Pulsed ASL (PICORE QT2) images were acquired on 3 T Siemens systems (TE/TR = 12/3400 msec, TI1/2 = 700/1900 msec).

Assessment: ASL-sCoV was calculated in temporal, parietal, occipital, and frontal lobes as well as whole gray matter.

Statistical Tests: The primary analysis used an analysis of covariance to investigate sCoV and cognitive group (CU, MCI, AD) associations. We also evaluated the repeatability of sCoV by calculating within-subject agreement in a subgroup of CU participants with a repeat ASL. The secondary analyses assessed ventricular volume, amyloid burden, glucose uptake, ASL-sCoV, and regional CBF as cognitive group classifiers using logistic regression models and receiver operating characteristic analyses.

Results: We found that global and temporal lobe sCoV differed between cognitive groups (P = 0.006). Post-hoc tests showed that temporal lobe sCoV was lower in CU than in MCI (Cohen's d = –0.36) or AD (Cohen's d = –1.36). We found that sCoV was moderately repeatable in CU (intersession intraclass correlation = 0.50; intrasession intraclass correlation = 0.88). Subsequent logistic regression analyses revealed that temporal lobe sCoV and amyloid uptake classified CU vs. MCI (P < 0.01; accuracy = 78%). Temporal lobe sCoV, amyloid, and glucose uptake classified CU vs. AD (P < 0.01; accuracy = 97%); glucose uptake significantly classified MCI vs. AD (P < 0.01; accuracy = 85%).

Data Conclusion: We showed that ASL spatial heterogeneity can be used alongside AD neuroimaging markers to distinguish cognitive groups, in particular, cognitively unimpaired from cognitively impaired individuals.

Level of Evidence: 2

Technical Efficacy: Stage 3

ALZHEIMER'S DISEASE (AD) is the most common type of dementia and for which, currently, there is no disease-modifying therapy available. Recent studies report that cerebral hemodynamic information provide some of the earliest signs of neurodegenerative processes that contribute to AD,[1,2] although the pathophysiological correlates remain a topic of debate. Early changes include inadequate cerebral blood flow (CBF) supply, microvascular dysfunction, altered

cerebral metabolism, or combinations thereof.[2] Cerebral hemodynamic measures offer potential as biomarkers for at-risk individuals, prior to AD diagnosis, which would enable screening and/or early interventions.

Arterial spin-labeled (ASL) magnetic resonance imaging (MRI) is well suited in this respect because it relies on a noninvasive endogenous tracer in the form of magnetically labeled blood water.[3] Previous ASL studies have shown reductions of global and regional CBF mainly in posterior cingulate cortex, precuneus, parietal lobes, and inferior frontal regions in patients with AD compared with cognitively unimpaired (CU) individuals.[4–7] Landau et al identified brain regions with abnormal glucose uptake in AD based on a meta-analysis; they found regions in posterior cingulate, temporal and parietal lobes, and called in meta-ROI (region of interest).[8] Given the relationship of glucose uptake and CBF, Wang et al used data from the Alzheimer's Disease Neuroimaging Initiative (ADNI) and found reduced CBF in meta-ROI in AD compared with CU.[9]

ASL is used primarily to image CBF; arterial transit time (ATT), however, is an additional source of hemodynamic contrast. For example, the intravascular ASL signal (ie, increased ASL signal in proximity to large vessels) produces angiographic contrast. Prolonged ASL-based ATT is prominent in aging[10,11] and AD[5] studies. ATT is easily measurable given additional scan time, but it is often omitted from clinical ASL studies in the interest of scan time.

Recent studies, however, shows that it is possible to estimate ATT indirectly from a single postlabeling delay ASL image, which is appealing clinically.[12,13] The spatial coefficient of variation (sCoV) across gray matter (GM) voxels is a single value that describes the spatial heterogeneity of CBF.[12] It is assumed that a CBF map that is relatively homogeneous across GM voxels will yield a low sCoV, and indicates a healthy perfusion pattern, whereas hemodynamic alterations that contribute to prolonged ATT and/or regional CBF changes will increase CBF spatial heterogeneity, thus increasing ASL sCoV. This study investigated the use of ASL sCoV in the classification of cognitively unimpaired and cognitively impaired individuals.

Materials and Methods

ADNI Dataset
Data used in the preparation of this article was obtained from the ADNI database (www.adni.loni.usc.edu). ADNI was launched in 2003 as a public–private partnership, led by Principal Investigator Michael W. Weiner, MD. The primary goal of ADNI has been to test whether serial MRI, positron emission tomography (PET), other biological markers and clinical and neuropsychological assessment can be combined to measure the progression of MCI and early AD. For up-to-date information, see www.adni-info.org.

Participants
Participants provided written informed consent and completed questionnaires approved by each participating site's Institutional Review Board. Participants were between 55 and 90 years old. They spoke English or Spanish fluently and had no contradiction to MRI. People with significant neurological disorders (other than AD) were excluded; this included major depression, bipolar disorder, schizophrenia, etc. The full list of inclusion/exclusion criteria for ADNI participants may be accessed at https://adni.loni.usc.edu/wp-content/uploads/2008/07/adni2-procedures-manual.pdf. Baseline data from ADNI-GO and ADNI-2 were used in the cross-sectional study since ADNI-1 did not include an ASL acquisition. Only CU, MCI, and AD cohorts were included. Early and late MCI groups were combined into a single MCI group. CU individuals were free of any memory impairment and any other significant impairment in cognitive function and activities of daily living. MCI and AD groups had abnormal memory function examined by the Wechsler memory scale and clinical dementia rating scores. A subgroup of CU who had a repeat scan in less than 3 months from baseline were also included for the repeatability analysis. Data collection occurred between April 2011 and January 2013 and data were accessed in June 2017. The sample sizes for secondary analysis were smaller, depending on the availability of other AD biomarkers.

MRI Acquisition
MR images were collected on 3 T Siemens (Erlangen, Germany) systems at 17 sites using a standardized protocol. Pulsed ASL (PICORE QT2) images were acquired with a 2D EPI readout with the following details: echo time (TE)/repetition time (TR) = 12/3400 msec, TI1/2 = 700/1900 msec, voxel size = 4 × 4 × 4 mm^3, and matrix size = 64 × 64 × 24. A total of 52 control-label pairs and an M0 calibration image were collected. 3D magnetization-prepared rapid gradient-echo (MPRAGE) T_1-weighted images were also acquired with TE = 3 msec, TR = 2300 msec, TI = 90 msec, flip angle = 9°, voxel size = 1 × 1 × 1.2 mm^3, and matrix = 256 × 240 × 176 for tissue segmentation purposes.

MRI Processing
We processed ASL images using the tools in the FMRIB software library.[14] This procedure consisted of: 1) aligning control and label images to the mean control image; 2) calculating the ASL difference images using sinc interpolation; 3) a quality control step acting on intermediate ASL difference images to increase the reliability of CBF estimates[15]; 4) calculating the average of ASL difference map from images that passed quality control; and 5) partial volume correction.[16] For CBF quantification, the following equation was used[3]:

$$CBF = 6000 \times \frac{\lambda \times \Delta M}{2 \times \alpha \times TI1 \times M0} \times e^{\frac{TI2 + \Delta t_z(z-1)}{T_{1,b}}} \qquad (1)$$

Where λ is the blood–brain partition coefficient (assumed to be 0.9 mL/g[17]); ΔM is the mean ASL difference image; α is the labeling efficiency (assumed to be 0.98[18]); TI1 and TI2 are ASL timing parameters (listed above); M0 is the ASL calibration image; $T_{1,b}$ is the longitudinal relaxation time of blood (assumed to be 1650 msec[19]); Δt_z is the acquisition time of each axial slice, and z is a slice number index.

Brain tissue segmentation was performed on the T_1-weighted image using FSL FAST[20] to isolate GM voxels based on a probability threshold of 70%. We coregistered T_1-weighted images to the

ASL coordinate space and overlaid the corresponding GM masks to CBF images using FSL FLIRT.[21] We calculated mean CBF (μ) and standard deviation of CBF across the voxels in the ROI (σ) to calculate ASL sCoV as the following (12):

$$\text{ASL sCoV}(\%) = \frac{\sigma}{\mu} \times 100 \qquad (2)$$

ASL sCoV generates one value per ROI with a higher value reflecting greater spatial heterogeneity.

Neuroimaging Summary Measures

We calculated ASL sCoV in frontal, temporal, parietal, and occipital lobes using the masks generated from the Harvard-Oxford atlas and coregistered to ASL space. For comparison, we also calculated ASL sCoV from all GM voxels, ie, a global measure of CBF spatial heterogeneity. As a summary measure of ASL CBF, we calculated mean CBF in the meta-ROI that was previously identified as affected regions in AD.[8,9]

We extracted ventricular and intracranial volumes from the processed MRI in the ADNI dataset; ventricular volume was calculated as described previously[22] and was normalized to the intracranial volume to serve as an index of brain tissue atrophy. We used Florbetapir PET processed data to represent the amyloid burden in the brain. The standardized uptake value ratio of amyloid was calculated as the following: mean uptake of cortical GM regions (including: frontal, anterior/posterior cingulate, lateral parietal, lateral temporal) divided by the mean uptake of cerebellum (ADNI_UCBERKELEY_AV45_Methods_12.03.15). From fluorodeoxyglucose PET, we used the average intensity normalized signal in the meta-ROI[8] as a proxy of cerebral glucose uptake.

Statistical Assessments

Statistical analyses were performed in R (R 3.3.3 GUI 1.66) with $P < 0.05$ defined as significant. For the primary analysis, we used an analysis of covariance in which sCoV was the dependent variable and cognitive group (CU, MCI, AD) was the independent variable. This analysis was repeated five times: four lobar ASL sCoV measures and one global GM; thus, the P-values were Bonferroni-corrected for multiple comparisons, ie, $P < 0.01$ was considered significant for these analyses. This primary model included these covariates: age, sex, APOE-ε4 status (APOE-ε4 noncarriers = 0; APOE-ε4 carriers = 1), number of retained ASL volumes, and site. The choice of covariates was based on previous studies that showed an effect of age and sex on ASL sCoV,[12] APOE-ε4 status on ASL measures,[23] and effect of site on ASL measures.[24] Lastly, the number of ASL volumes will vary by virtue of the image processing; thus, we control for calculating the ASL sCoV. We compared these measures' effect size by calculating a Cohen's d to identify the most pertinent ASL sCoV metric, ie, global or lobar sCoV.

In the repeatability analysis, we conducted paired-sample t-tests and calculated the intraclass correlation coefficient (ICC) between the baseline and repeat ASL sCoV in global GM. For this analysis, ASL sCoV measures were not adjusted for any of the above-mentioned covariates to avoid any potential bias in the repeatability estimates. We also performed an intrasession repeatability analysis: ASL sCoV was calculated twice per participant by splitting the ASL difference images at baseline into two independent sets and comparing the sCoV estimates.

The secondary analyses assessed normalized ventricular volume, amyloid burden, glucose uptake, ASL sCoV, and meta-ROI CBF as cognitive group classifiers using logistic regression models, with age, sex, and APOE-ε4 as covariates. The choice of covariates for the secondary analysis was based on previous studies that showed effects of age, sex, and APOE-ε4 status on AD diagnosis.[25,26] Neuroimaging measures were tested and adjusted for the site effect when necessary, prior to the classification analysis, by calculating the residuals using analysis of variance models.

We then performed receiver operating characteristic analyses and calculated maximum accuracy as well as area under the curve to indicate the performance of models with and without ASL measures. To examine the added value of ASL measures statistically, we conducted likelihood ratio tests with $P < 0.05$ defined as significant.

Results

Table 1 summarizes the sample characteristics for the primary analysis. A sample of 258 individuals was available for the primary analysis; a subsample of 159 individuals had additional neuroimaging measures required for the secondary analysis. Each ASL image includes 104 intermediate ASL difference images obtained from 52 control-label pairs. A quality control procedure was performed to exclude poor-quality intermediate ASL difference images.[15] After the quality control step, the number of retained ASL difference images in this sample ranged from 31 to 103 out of the possible 104 intermediate images (mean = 84; SD = 14). Figure 1 shows three representative CBF maps from the participants in this study with their corresponding density plots of voxel intensities in GM. These plots show that higher sCoV corresponds to more intravascular artifact and more skewed CBF histograms.

Figure 2 illustrates ASL sCoV measures with respect to the cognitive groups. Analysis of covariance revealed that global GM sCoV ($F_{2,258} = 5.2$, $P = 0.006$) as well as sCoV in temporal lobe ($F_{2,258} = 5.1$, $P = 0.006$) differed between cognitive groups after adjusting for primary covariates. Table 2 shows between-group effect sizes of temporal sCoV and total GM. The temporal lobe sCoV had a greater effect size compared with global sCoV, thus this lobar ROI was used for the secondary analysis.

To assess reproducibility of the ASL sCoV metric, baseline and 3-month repeat ASL scans were considered from 39 available CU participants. Figure 3a,b shows the scatterplot and Bland–Altman plot for ASL sCoV, respectively (colors denote site). One case was removed from the repeatability analysis due to an artifact in the repeat ASL image, and marked with an asterisk in the plots. We found there was no significant difference between baseline and repeat sCoV measures (paired t-test; $P > 0.2$; Cohen's d = –0.22). In addition, there was a moderate agreement[27] between these two measurements (ICC = 0.50; $N = 38$).

TABLE 1. Sample Characteristics of the Primary Analysis (N = 258)			
Parameters	CU (*n* = 67)	MCI (*n* = 156)	AD (*n* = 35)
Age (years)	74.1 (56.3–87.6)	71.8 (55.1–85.7)	76.6 (56.3–88.9)
Sex (male/female)	35; 32	88; 68	21; 14
MMSE (max:30)	28.9 (24–30)	27.8 (19–30)	22.6 (19–26)
APOE-ε4 (+/-)	17; 50	83; 73	19; 16
Gray matter ASL sCoV (%)	73.4 (41.3–207.6)	84.0 (42.6–234.2)	91.2 (53.0–267.2)
Meta-ROI CBF (mL/100 g/min)	84.0 (25.3–236.4)	77.8 (13.1–170.4)	67.9 (36.8–126.6)

Mean (range) or counts are reported.
CU: cognitively unimpaired; MCI: mild cognitive impairment; AD: Alzheimer's disease; MMSE: mini-mental state examination; *APOE*-ε4: Apolipoprotein E4; sCoV: spatial coefficient of variation; CBF: cerebral blood flow.
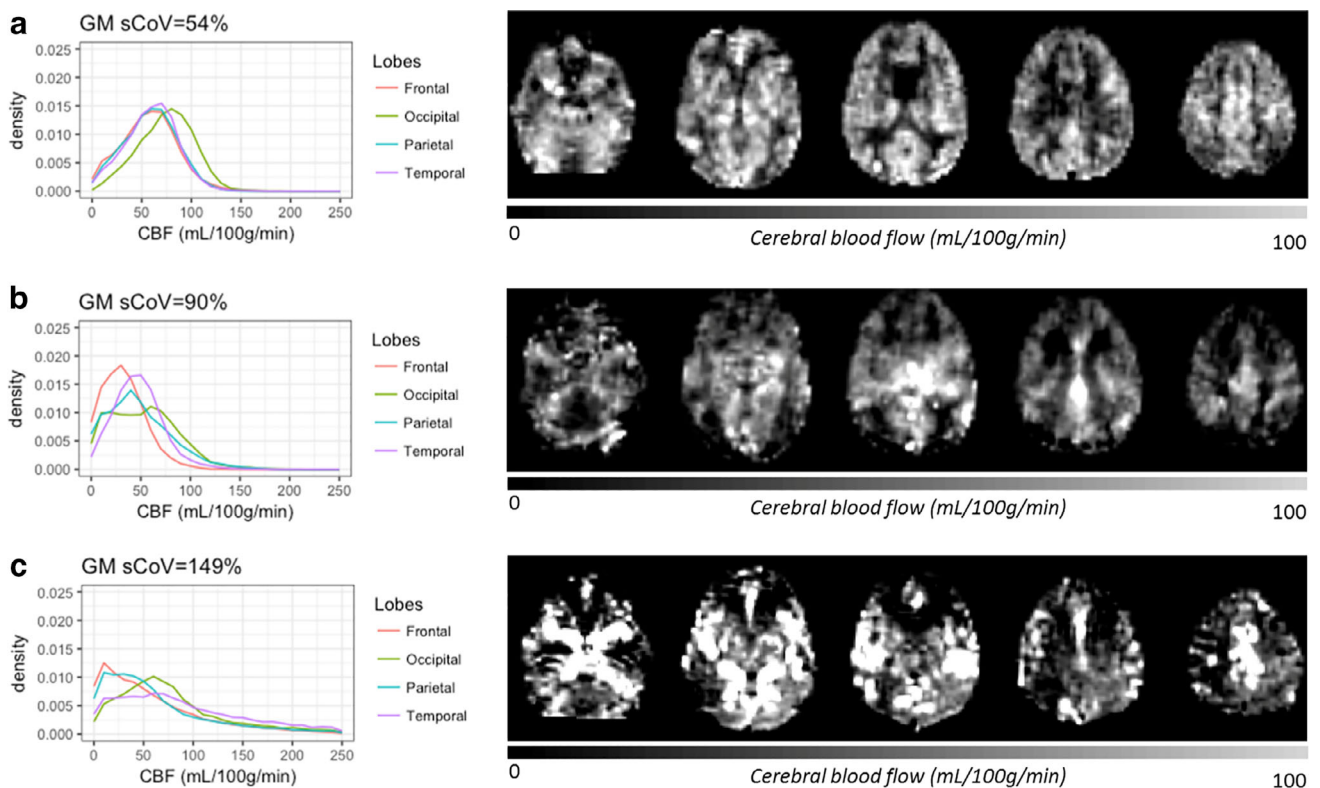
FIGURE 1: Left: Density plots of ASL CBF voxels for three representatives with low (a), intermediate (b), and high (c) spatial heterogeneity. Right: Corresponding CBF images are shown in 2 × 2 × 2 mm³ Montreal Neurological Institute (MNI152) standard space.

For the intrasession repeatability, we used baseline ASL data from 39 CU individuals, ie, two CBF maps and two sCoV values for these participants. The scatter and Bland–Altman plots show no intrasession difference in sCoV (Fig. 3c,d, where colors denote site). We found there was no significant difference between these two sCoV measures (paired *t*-test; $P > 0.6$; Cohen's d = –0.23). In addition, there was a high agreement[27] between these two measurements (ICC = 0.88; N = 39).

Table 3 summarizes the neuroimaging measures in three cognitive groups. Table 4 shows logistic regression results for CU vs. MCI, CU vs. AD, and MCI vs. AD. Odds ratio and z values are reported for each classifier. Odds ratios that are significantly greater than 1 correspond to significant classifiers. The z values are reported to show the directionality of the classifiers, ie, classifiers with positive z values were elevated in the cognitively impaired group compared with less impaired group, whereas negative z values corresponded to

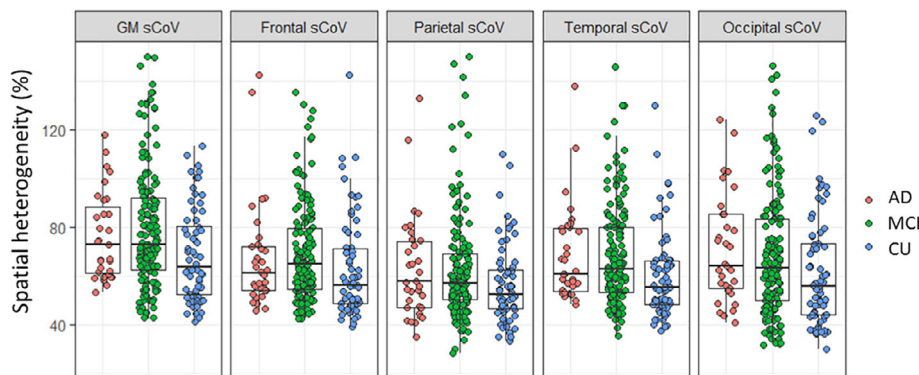**FIGURE 2:** Spatial heterogeneity of ASL CBF images for the different cognitive groups: CU, MCI, and AD. GM sCoV (*P* = 0.006) and temporal lobe sCoV (*P* = 0.006) were significantly different between groups.

TABLE 2. Effect Sizes (Cohen's d) Are Calculated to Show Pairwise Group Differences in sCoV for Two of the Five Brain Regions Investigated

Cognitive groups	Gray matter sCoV	Temporal lobe sCoV
CU vs. MCI	**−0.32***	**−0.36***
CU vs. AD	**−0.63***	**−1.36***
MCI vs. AD	−0.16	−0.20

*Significant *P* values at *P* < 0.01 (*P* value is Bonferroni corrected for five comparisons).
CU: cognitively unimpaired; MCI: mild cognitive impairment; AD: Alzheimer's disease; sCoV: spatial coefficient of variation.

reduced values in the cognitively impaired group. For CU vs. MCI, the temporal lobe sCoV and amyloid burden classified these two groups with 78% accuracy. For CU vs. AD, the amyloid burden, glucose uptake, and temporal lobe sCoV classified these two groups with 97% accuracy. For MCI vs. AD, the meta-ROI glucose uptake classified these two groups with 85% accuracy.

The receiver operating characteristic analyses results are summarized in Fig. 4. Area under the curve and maximum accuracy are indicated in each curve. Models in which ASL added value to other neuroimaging measures in cognitive group classification are marked with an asterisk (likelihood ratio test, *P* < 0.05). ASL measures added value in all the CU vs. MCI classification models. ASL measures also added value to all but glucose included CU vs. AD classification models.

Discussion

This study demonstrates that temporal lobe spatial heterogeneity of ASL CBF can be used to effectively classify cognitive groups, namely because this convenient ASL metric distinguished CU from MCI and AD groups. Used in concert with other neuroimaging markers (ie, neuroanatomical volumes,

regional CBF, amyloid burden, and glucose uptake), CBF spatial heterogeneity contributed to group classifications between 78% to 97% in accuracy.

The results of the current study are in line with previous ASL research that show associations between CBF and/or ATT with cognitive group.[5,9] The current study, however, used sCoV as a proxy for ATT and it was calculated from a single postlabel delay ASL acquisition. Vascular dysregulation is posited to be an early AD marker,[1] which is consistent with the results presented in the current study. We found that sCoV was different between cognitively unimpaired and cognitively impaired groups but not between MCI and AD. This suggests sCoV may be better suited to track hemodynamic changes that happen at an earlier phase of AD progression. We speculate that the lack of significant finding between MCI and AD may be because more vascular dysregulation is less remarkable as neurodegeneration advances or that more widespread regional CBF reductions acts as a competing source of sCoV contrast; mechanisms that govern this image contrast remain unresolved. Further work is needed to resolve the competing sources of contrast in CBF data broadly and their influences on the sCoV summary measure.

The choice of MRI pulse sequence parameters dictates the dominant source of contrast in an ASL image. The sCoV can be calculated for an ASL difference image. For an ASL acquisition with long postlabeling delays (>2000 msec), the tracer signal is more likely to reside in the tissue, so that the corresponding sCoV is expected to be low and represent spatial variability of perfusion. For an ASL acquisition with shorter postlabeling delays (<1500 msec), the tracer is more likely to reside within large arteries, thus producing angiographic image contrast and contribute to a higher spatial heterogeneity (ie, sCoV) effect, akin to ATT artifacts.[3] Using a modified ASL sequence, ie, one that suppresses large vessel signal with vascular crushing gradients,[28] it may be possible to disentangle the competing sources of sCoV. The postlabeling delay for the ADNI ASL was relatively short (1200 msec), below the recommended range established after the ADNI ASL protocol was devised (1800–2000 msec).[3] This helps to
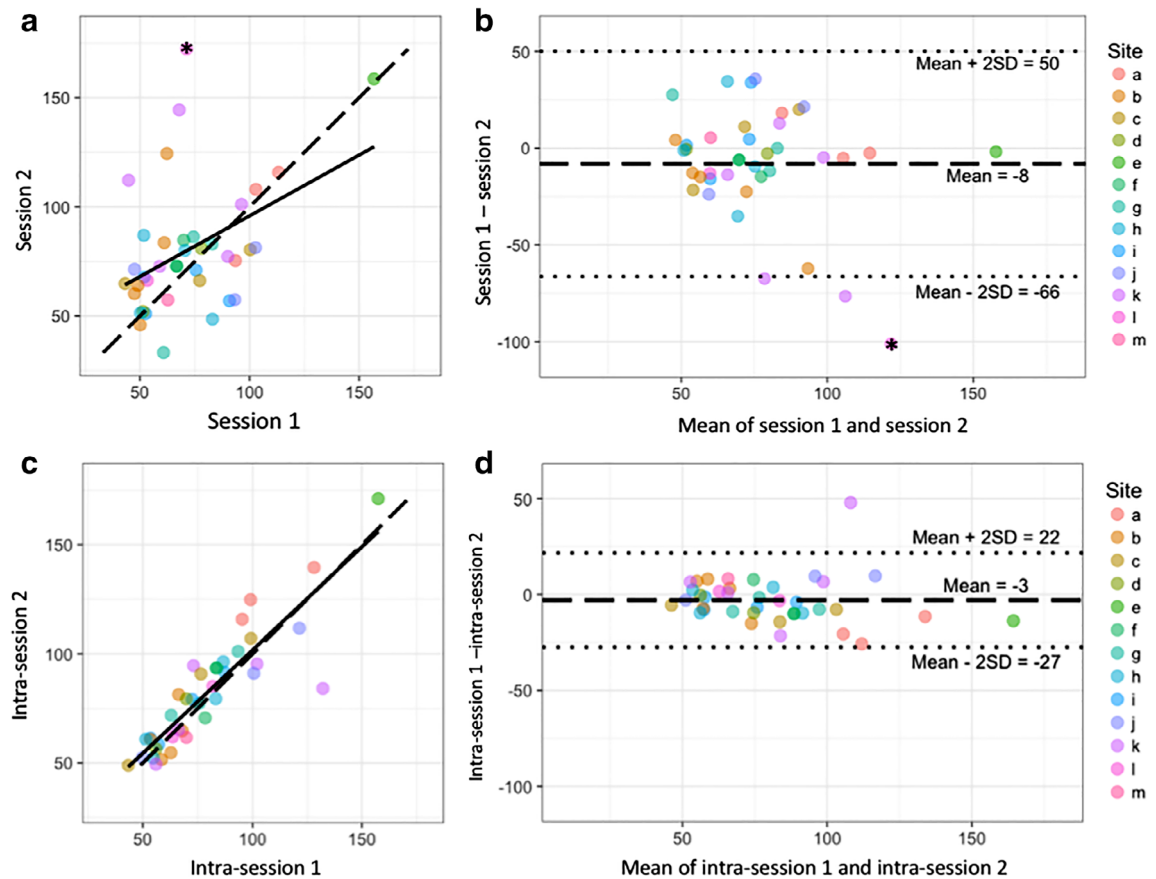
FIGURE 3: a: Scatterplot of ASL sCoV at session 1 and session 2. Solid line shows the regression line of session 1 and session 2 and dashed line shows the equality line for reference. b: Bland–Altman plot for the baseline (session 1) and 3-month repeat (session 2) ASL sCoV. c: Scatterplot of ASL sCoV for intrasession 1 and intrasession 2 obtained from intrasession repeatability analysis. Solid line shows the regression line and dashed line shows the equality line for reference. d: Bland–Altman plot for the intrasession ASL sCoV. The dashed lines in B and D show the mean of difference and dotted lines show mean ± 2 × SD of difference. Data are labeled by site while the site ID is recoded.

TABLE 3. Sample Characteristics of the Secondary Analysis (*N* = 159)			
Parameters	**CU (*n* = 41)**	**MCI (*n* = 88)**	**AD (*n* = 30)**
Age (years)	73.5 (63.2–84.7)	71.0 (55.1–85.1)	76.4 (62.3–86.6)
Sex (male/female)	19; 22	39; 49	19; 11
MMSE (max:30)	28.8 (24–30)	28.1 (24–30)	22.9 (19–26)
APOE-ε4 (+/-)	12; 29	45; 43	18; 12
Gray matter ASL sCoV (%)	72.7 (43.2–207.5)	83.3 (45.1–210.4)	85.0 (53.0–211.8)
Meta-ROI CBF (mL/100 g/min)	81.7 (25.3–236.4)	78.5 (13.1–142.6)	70.2 (36.8–126.6)
Ventricular volume (%ICV)	3.5 (0.9–9.2)	3.9 (0.9–11.6)	4.8 (1.8–10.5)
Amyloid burden (SUVR)	1.1 (0.9–1.7)	1.2 (0.8–2.0)	1.3 (0.8–1.7)
Meta-ROI Glucose uptake (SUVR)	1.3 (1.1–1.5)	1.2 (0.9–1.6)	1.1 (0.8–1.3)

Secondary analysis is a subgroup of the primary analysis for which neuroimaging measures in addition to ASL were available. Mean (range) or counts are reported.
CU: cognitively unimpaired; MCI: mild cognitive impairment; AD: Alzheimer's disease; sCoV: spatial coefficient of variation; CBF: cerebral blood flow; ICV: intracranial volume; SUVR: standardized uptake value ratio.

TABLE 4. Results of Logistic Regression Models to Classify Cognitive Groups

Neuroimaging markers	CU vs. MCI	CU vs. AD	MCI vs. AD
Ventricular volume (%ICV)	1.02 (1.7)	1.02 (.56)	1.0 (1.5)
Amyloid burden (SUVR)	*1.35* (2.38)	*5.6* (2.26)	1.1 (1.1)
Meta-ROI Glucose uptake (SUVR)	1.15 (–.76)	*60.1* (–2.26)	*2.7* (–3.8)
Meta-ROI ASL CBF (mL/100 g/min)	1.03 (.5)	1.02 (–.2)	1.1 (–1.5)
Temporal lobe ASL sCoV (%)	*1.16* (2.47)	*1.8* (2.0)	1.0 (.4)
Overall model accuracy	78%	97%	85%

Odds ratio (z values) are reported.
*Significant P values at $P < 0.05$.
CU: cognitively unimpaired; MCI: mild cognitive impairment; AD: Alzheimer's disease; sCoV: spatial coefficient of variation; CBF: cerebral blood flow; ICV: intracranial volume; SUVR: standardized uptake value ratio.

explain why the range of GM sCoV in this study was higher than what was found previously in a group of elderly participants. The postlabeling delay in the previous study was longer (1525 msec); therefore, we would expect more intravascular sources in ADNI ASL data, and hence higher sCoV.[12] In addition, ADNI used a pulsed ASL acquisition, while Mutsaerts et al[12] used a pseudocontinuous ASL, and this could explain the differences between the two studies.[3]

Although we found that ASL sCoV has a moderate repeatability in CU individuals within a 3-month time window,[27] the intrasession analysis showed that ASL sCoV has a high repeatability. The intersession ASL repeatability coefficient was lower in this study compared with previous reports on ASL ATT and CBF.[24] There might be several explanations for this, including: 1) ASL repeatability studies are usually performed within a 1- or 2-week time window, whereas baseline and repeat visits were 3 months apart in this study; and 2) the Bland–Altman plot also suggests some sites had lower reproducibility. This was also observed in the previous ASL repeatability study in which ICC ranged from 0.07–0.78 among 28 different sites. The sample size of the current study, however, was not sufficient to explore site effect statistically, ie, $N = 39$ from 13 sites. The site reproducibility discrepancies might relate to variability in subject compliance (ie, vigilance to remain still during scanning), subject positioning in the scanner, and/or operator-dependent planning of ASL images.

The results from the current study showed that ASL sCoV was able to classify CU vs. MCI and CU vs. AD while accounting for additional neuroimaging metrics: ventricular volume, amyloid burden, and glucose uptake. Classification accuracy obtained from these models (CU vs. MCI: 78%; CU vs. AD: 97%; MCI vs. AD: 85%) were a few percentage points higher than previous reports of comparable sample sizes. Apostolova et al reported an accuracy of CU vs. MCI: 77%; CU vs. AD: 84%; MCI vs. AD: 69% using anatomical

MRI and cerebrospinal fluid markers.[25] Another study reported 62.7% accuracy in classification of CU, MCI, and AD using anatomical features that included hippocampal shape, texture, and cortical thickness.[29] A whole-brain hierarchical network analysis of >700 brain images showed accuracy of CU vs. MCI: 84%; CU vs. AD: 94%; MCI vs. AD: 88%.[30] On the other hand, Wang et al showed that the meta-ROI ASL CBF was significantly reduced in AD compared with CU; their model did not include structural, glucose, nor amyloid markers.[9] Given the significant role of other imaging markers, we speculate that our study presents comprehensive classification models, and demonstrates the unique contributions provided by the different AD markers. Moreover, Bron et al observed that regional CBF did not significantly improve the classification accuracy of CU vs. AD after accounting for structural markers.[31] This is in line with our results and supports the use of ASL sCoV as a classifier of CU from cognitively impaired cohorts.

Our results suggest that cerebral hemodynamic alterations represent a useful element in assessing AD profiles, independent of structural, amyloid burden, or glucose uptake abnormalities. A recent study found that extracranial blood velocity is inversely related to ASL sCoV[32]; which unfortunately was not possible to evaluate in the current study because phase contrast angiography from external arteries was not collected. Future studies are required to disambiguate large-artery from small-vessel hemodynamic influences on the ASL sCoV metric. Hemodynamic changes in AD are thought to reflect: 1) cerebral amyloid angiopathy[33]; 2) pericyte degeneration which is associated with capillary reduction and tortuosity of vessels[34,35]; and/or 3) vascular alterations such as arterial stiffness, atherosclerosis, and vessel thrombi or hemorrhage.[26] A transgenic AD mouse model supports that these hemodynamic features as microvascular impairments due to cerebral amyloid angiopathy contributed to prolonged ATT.[36] An [15]O PET-ASL comparison study shows
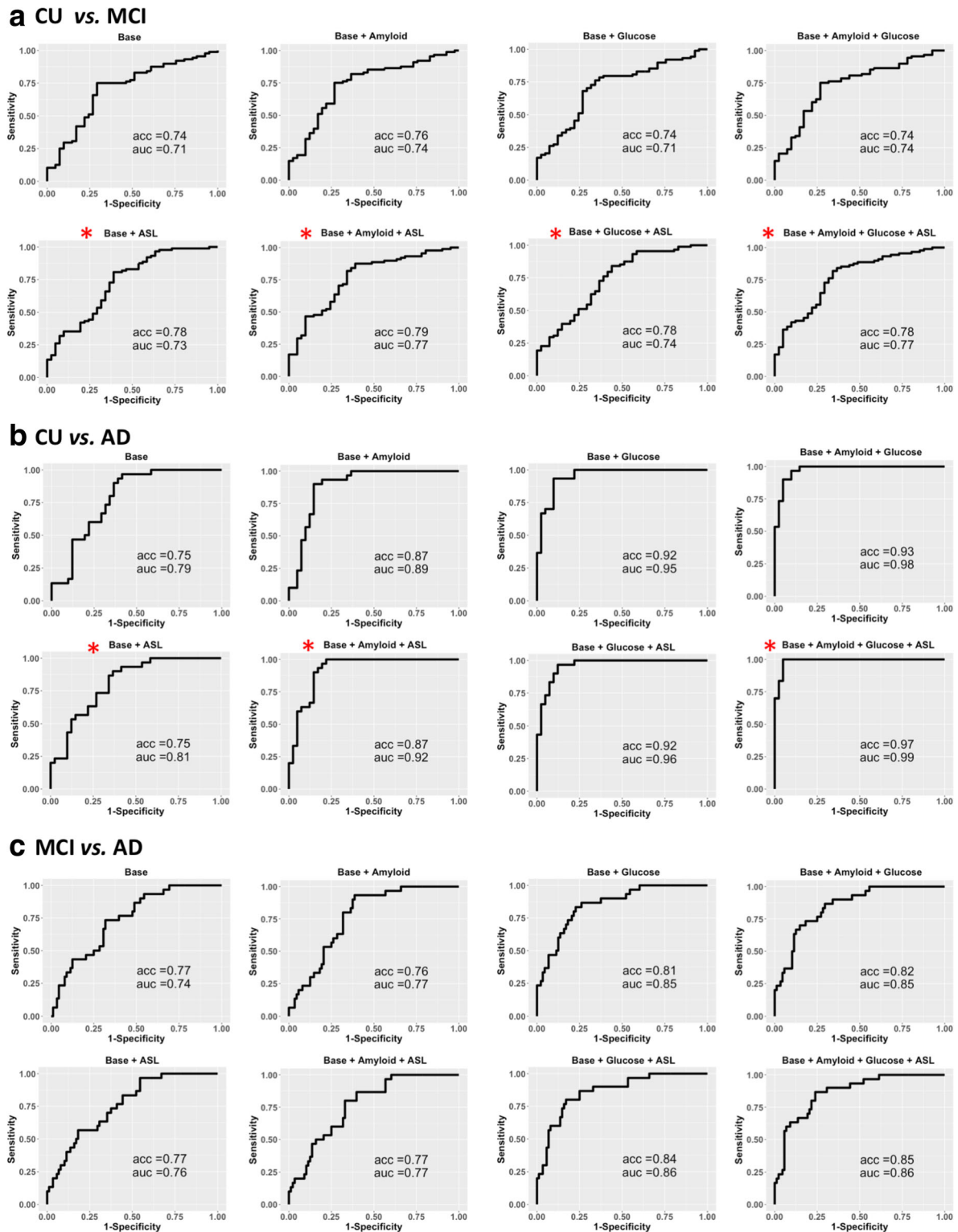
FIGURE 4: Receiver operating characteristics curves for different classifiers. Accuracy (acc) and area under the curve (AUC) are provided for reference. (a) CU vs. MCI, (b) CU vs. AD, and (c) MCI vs. AD. The base model consisted of age, sex, APOE-ε4, and ventricular volume. ASL features include mean CBF in meta-ROI and temporal lobe sCoV. Glucose: glucose uptake from fluorodeoxyglucose PET. Amyloid: amyloid burden from Florbetapir PET. *ASL measures added value to the cognitive group classification (likelihood ratio test at P < 0.05).

that ASL sCoV negatively relates to resting CBF and CBF response to hypercapnia.[13] It remains to be seen whether cerebral amyloid angiopathy is one source of the elevated sCoV and this may be a fruitful area of future work.

Pathological findings show that amyloid deposition in the form of cerebral amyloid angiopathy is spatially heterogeneous.[37] A more recent study showed that severity of cerebral amyloid angiopathy is related to hippocampal microinfarcts

and cognitive dysfunction.[38] We therefore speculate that the temporal lobe is more susceptible to these hemodynamic alterations and this may explain why we observed a greater effect size for temporal sCoV compared with global GM sCoV in classifying CU vs. AD. ASL sCoV can, therefore, be used to describe the severity of hemodynamic-related abnormalities associated with AD. This summary metric may be added to a multicontrast MRI session for screening and monitoring people at risk of AD. In particular, it could serve as a response measure for interventions that target physiological abnormalities.

This study has some limitations. Although previous work shows that ASL sCoV shares >70% variance with ATT,[12] other sources could contribute to the spatial heterogeneity of the ASL. These include ASL artifacts from head motion, partial volume effects, susceptibility-induced distortions, and site effects. To reduce image artifacts, we used a recently developed pipeline (ENABLE) that identifies and excludes poor-quality intermediate ASL difference images and optimized for the chosen postlabeling delay.[15] To address partial volume effects, we corrected ASL CBF maps using tissue segmentation maps obtained from structural images.[16] ASL images in this study were not corrected for susceptibility artifacts, as only a single proton density image was collected. Others have reported that susceptibility effects can be corrected.[39] Madai et al found that, while correction for susceptibility artifacts improved the similarity between ASL and dynamic susceptibility contrast CBF maps, it did not have any influence on the appearance of intravascular artifact owing to increased ATT in patients with cerebrovascular disease.[39] Therefore, we speculate that this does not influence the role of ASL sCoV in cognitive group classification. To account for a potential confounding effect of site, ASL measures were adjusted. Site effects may be due to between-site participant selection bias[40] or scan prescription systematic differences, such as the placement of ASL labeling and imaging regions.

Moreover, CBF quantification parameters, such as labeling efficiency, relaxation time of blood, and the blood–brain partition coefficient were assumed to be constant among cohorts, since these measurements were not performed in ADNI. Future research may investigate the effect of these parameters on ASL measures in different cohorts. However, the effects of these parameters can be expected to be equal across the brain. Therefore, they are not expected to have a significant effect on sCoV, which is only influenced by effects that vary across the brain. Another avenue for future work is to study sCoV in different brain regions, ie, smaller regions of interest, or studying the vascular territories separately. Another aspect of the sCoV signal that remains unresolved is what happens if the labeling plane is made more proximal or distal from the imaging volume, as this could influence sCoV. Furthermore, it is currently not possible to comment on whether the cardiac output or heart rate, each yielding some influence on the volume of blood moving into the brain, would influence sCoV.

In conclusion, we showed that the ASL spatial heterogeneity differs among cognitive groups, CU, MCI, and AD. ASL sCoV indexes delayed blood delivery and/or regional perfusion changes and is extracted from a single postlabeling delay ASL acquisition without any additional scans or postprocessing. This ASL metric added value in classification of CU vs. MCI and AD to established AD markers, emphasizing ASL as a noninvasive vascular imaging marker of AD.

References

1. Iturria-Medina Y, Sotero RC, Toussaint PJ, Mateos-Perez JM, Evans AC, Alzheimer's Disease Neuroimaging Initiative. Early role of vascular dysregulation on late-onset Alzheimer's disease based on multifactorial data-driven analysis. Nat Commun 2016;7:11934.

2. Nelson AR, Sweeney MD, Sagare AP, Zlokovic BV. Neurovascular dysfunction and neurodegeneration in dementia and Alzheimer's disease. Biochim Biophys Acta Mol Basis Dis 2016;1862:887–900.

3. Alsop DC, Detre JA, Golay X, et al. Recommended implementation of arterial spin-labeled perfusion MRI for clinical applications: A consensus of the ISMRM Perfusion Study group and the European consortium for ASL in dementia. Magn Reson Med 2015;73:102–116.

4. Asllani I, Habeck C, Scarmeas N, Borogovac A, Brown TR, Stern Y. Multivariate and univariate analysis of continuous arterial spin labeling perfusion MRI in Alzheimer's disease. J Cereb Blood Flow Metab 2008;28:725–736.

5. Mak HKF, Chan Q, Zhang Z, et al. Quantitative assessment of cerebral hemodynamic parameters by QUASAR arterial spin labeling in Alzheimer's disease and cognitively normal Elderly adults at 3-Tesla. J Alzheimers Dis 2012;31:33–44.

6. Okonkwo OC, Xu G, Oh JM, et al. Cerebral blood flow is diminished in asymptomatic middle-aged adults with maternal history of Alzheimer's disease. Cereb Cortex 2014;24:978–988.

7. Yoshiura T, Hiwatashi a, Yamashita K, et al. Simultaneous measurement of arterial transit time, arterial blood volume, and cerebral blood flow using arterial spin-labeling in patients with Alzheimer disease. AJNR Am J Neuroradiol 2009;30:1388–1393.

8. Landau SM, Harvey D, Madison CM, et al. Associations between cognitive, functional, and FDG-PET measures of decline in AD and MCI. Neurobiol Aging 2011;32:1207–1218.

9. Wang Z, Das SR, Xie SX, Arnold SE, Detre JA, Wolk DA. Arterial spin labeled MRI in prodromal Alzheimer's disease: A multi-site study. NeuroImage Clin 2013;2:630–636.

10. Dai W, Fong T, Jones RN, et al. Effects of arterial transit delay on cerebral blood flow quantification using arterial spin labeling in an elderly cohort. J Magn Reson Imaging 2017;45:472–481.

11. Liu Y, Zhu X, Feinberg D, et al. Arterial spin labeling MRI study of age and gender effects on brain perfusion hemodynamics. Magn Reson Med 2012;68:912–922.

12. Mutsaerts HJ, Petr J, Václavů L, et al. The spatial coefficient of variation in arterial spin labeling cerebral blood flow images. J Cereb Blood Flow Metab 2017;37:3184–3192.

13. Ibaraki M, Nakamura K, Toyoshima H, et al. Spatial coefficient of variation in pseudo-continuous arterial spin labeling cerebral blood flow images as a hemodynamic measure for cerebrovascular steno-occlusive disease: A comparative 15O positron emission tomography study. J Cereb Blood Flow Metab 2018;271678X18781667.

14. Jenkinson M, Beckmann CF, Behrens TEJ, Woolrich MW, Smith SM. FSL. Neuroimage 2012;62:782–790.

15. Shirzadi Z, Stefanovic B, Chappell MA, et al. Enhancement of automated blood flow estimates (ENABLE) from arterial spin-labeled MRI. J Magn Reson Imaging 2018;47:647–655.

16. Chappell MA, Groves AR, MacIntosh BJ, Donahue MJ, Jezzard P, Woolrich MW. Partial volume correction of multiple inversion time arterial spin labeling MRI data. Magn Reson Med 2011;65:1173–1183.

17. Herscovitch P, Raichle ME. What is the correct value for the brain—blood partition coefficient for water? J Cereb Blood Flow Metab 1985;5:65–69.

18. Wong EC, Buxton RB, Frank LR. A theoretical and experimental comparison of continuous and pulsed arterial spin labeling techniques for quantitative perfusion imaging. Magn Reson Med 1998;40:348–355.

19. Lu H, Clingman C, Golay X, van Zijl PCM. Determining the longitudinal relaxation time (T1) of blood at 3.0 Tesla. Magn Reson Med 2004;52:679–682.

20. Smith SM. Fast robust automated brain extraction. Hum Brain Mapp 2002;17:143–155.

21. Jenkinson M, Bannister P, Brady M, Smith S. Improved optimization for the robust and accurate linear registration and motion correction of brain images. Neuroimage 2002;17:825–841.

22. Nestor SM, Rupsingh R, Borrie M, et al. Ventricular enlargement as a possible measure of Alzheimer's disease progression validated using the Alzheimer's disease neuroimaging initiative database. Brain 2008;131:2443–2454.

23. de la Torre JC. Genetics of Alzheimer's disease. In: *Alzheimer's turn point*. Cham, Switzerland: Springer International Publishing; 2016:75–83.

24. Petersen ET, Mouridsen K, Golay X. The QUASAR reproducibility study. Part II: Results from a multi-center Arterial Spin Labeling test-retest study. Neuroimage 2010;49:104–113.

25. Apostolova LG, Hwang KS, Kohannim O, et al. ApoE4 effects on automated diagnostic classifiers for mild cognitive impairment and Alzheimer's disease. NeuroImage Clin 2014;4:461–472.

26. de la Torre JC. Conditions that can promote Alzheimer's. In: *Alzheimer's turn point*. Cham, Switzerland: Springer International Publishing; 2016:99–150.

27. Koo TK, Li MY. A guideline of selecting and reporting intraclass correlation coefficients for reliability research. J Chiropr Med 2016;15:155–163.

28. Wang J, Alsop DC, Song HK, et al. Arterial transit time imaging with flow encoding arterial spin tagging (FEAST). Magn Reson Med 2003;50:599–607.

29. Sørensen L, Igel C, Pai A, et al. Differential diagnosis of mild cognitive impairment and Alzheimer's disease using structural MRI cortical thickness, hippocampal shape, hippocampal texture, and volumetry. NeuroImage Clin 2017;13:470–482.

30. Liu J, Li M, Lan W, Wu F-X, Pan Y, Wang J. Classification of Alzheimer's disease using whole brain hierarchical network. IEEE/ACM Trans Comput Biol Bioinforma 2018;15:624–632.

31. Bron EE, Steketee RME, Houston GC, et al. Diagnostic classification of arterial spin labeling and structural MRI in presenile early stage dementia. Hum Brain Mapp 2014;35:4916–4931.

32. Robertson AD, Matta G, Basile VS, et al. Temporal and spatial variances in arterial spin-labeling are inversely related to large-artery blood velocity. AJNR Am J Neuroradiol 2017;38:1555–1561.

33. Lai AY, Dorr A, Thomason LAM, et al. Venular degeneration leads to vascular dysfunction in a transgenic model of Alzheimer's disease. Brain 2015;138(Pt 4):1046–1058.

34. Winkler EA, Sagare AP, Zlokovic BV. The pericyte: A forgotten cell type with important implications for Alzheimer's disease? Brain Pathol 2014;24:371–386.

35. Montagne A, Nikolakopoulou AM, Zhao Z, et al. Pericyte degeneration causes white matter dysfunction in the mouse central nervous system. Nat Med 2018;24:326–337.

36. Dorr A, Sahota B, Chinta LV, et al. Amyloid-β-dependent compromise of microvascular structure and function in a model of Alzheimer's disease. Brain 2012;135(Pt 10):3039–3050.

37. Allen N, Robinson AC, Snowden J, Davidson YS, Mann DMA. Patterns of cerebral amyloid angiopathy define histopathological phenotypes in Alzheimer's disease. Neuropathol Appl Neurobiol 2014;40:136–148.

38. Hecht M, Krämer LM, von Arnim CAF, Otto M, Thal DR. Capillary cerebral amyloid angiopathy in Alzheimer's disease: Association with allocortical/hippocampal microinfarcts and cognitive decline. Acta Neuropathol 2018;135:681–694.

39. Madai VI, Martin SZ, von Samson-Himmelstjerna FC, et al. Correction for susceptibility distortions increases the performance of arterial spin labeling in patients with cerebrovascular disease. J Neuroimaging 2016;26:436–444.

40. Ramirez J, McNeely AA, Scott CJM, Masellis M, Black SE. Alzheimer's Disease Neuroimaging Initiative: White matter hyperintensity burden in elderly cohort studies: The Sunnybrook Dementia Study, Alzheimer's Disease Neuroimaging Initiative, and Three-City Study. Alzheimer's Dement 2016;12:203–210.